SAND2022-5888C

The geologic framework of the West Flank of Coso FORGE site

Drew L. Siler, Kelly Blake, Andrew Sabin, Mike Lazaro, Dave Meade, Douglas Blankenship, B. Mack Kennedy, Jess McCulloch, Steve DeOreo, Stephen Hickman, Jonathan Glen, Ole Kaven, Martin Schoenball, Colin Williams, Geoff Phelps, James E. Faulds, Nicholas H. Hinz,, Ann Robertson-Tait

[1]Lawrence Berkeley National Laboratory, Berkeley, California
[2]U.S. Navy Geothermal Program Office, China Lake, 93555
[3]Sandia National Laboratories, Albuquerque, New Mexico 87185
[4]Coso Operating Company LLC, Coso Junction, 93542
[5]U.S. Geological Survey, Menlo Park, California
[6]Nevada Bureau of Mines and Geology, University of Nevada, Reno, Nevada 89557
[7]Department of Geological Sciences and Engineering, University of Nevada, Reno 89557
[8]GeothermEx/Schlumberger

Keywords: West Flank, Coso, FORGE, EGS, structure, geology

ABSTRACT

The proposed West Flank FORGE site is located immediately west and outside of the Coso geothermal field on Naval Air Weapons Station China Lake in eastern, CA. Data confirm that the West Flank site consists of predominantly crystalline granitic rocks, with low permeability, and temperatures in excess of 175°C at ~1.7 km beneath the surface. Well testing data confirm that the West Flank site is not hydrologically connected to the neighboring Coso geothermal field. Stress data suggest that the natural fracture system is well oriented for reactivation during EGS stimulation. The 3D geologic framework model for West Flank confirms that these characteristics are present in the subsurface throughout the site, and indicate that a minimum volume of ~2.5 km^3 rock satisfy FORGE criteria within 4 km of the surface. As such the proposed West Flank site represents an ideal environment for development, testing, and validation of EGS technologies under the FORGE initiative.

1. INTRODUCTION

The Department of Energy (DOE) Frontier Observatory for Research in Geothermal Energy (FORGE) project is designed to test and report on techniques needed to make Enhanced Geothermal Systems (EGS) a commercially viable electricity generation option for the United States. The objective of FORGE is to establish and manage a dedicated site where the scientific and engineering community can develop, test, and improve new technologies in an environment that is well characterized and instrumented, and has optimal target reservoir temperature, depth, lithology, and permeability for EGS. Here we present the geologic framework of the proposed West Flank FORGE site as interpreted through integration of a wide variety of existing geologic, geophysical, and geochemical data. These data, which include lithologic data form ~15,000 m of core and well cuttings from boreholes in and around the site, stress data, thermal data, well-test data, geochemistry data, alteration data, gravity and magnetic data, magnetotelluric data, and interpreted seismic reflection profiles were compiled into a 3D geologic framework model of the West Flank Site.

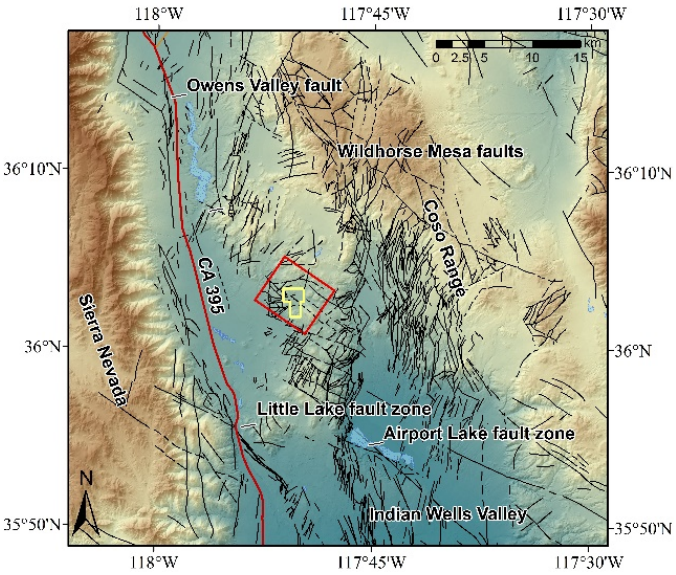

Figure 1. Regional map of the Coso Range/Indian Wells Valley area. Faults from USGS Quaternary fault and fold data base. Yellow polygon indicates the proposed West Flank FORGE site, red box is the extent of the 3D geologic model.

The above data, in conjunction with the 3D geologic framework model, confirm that the West Flank site meets all criteria established by DOE for the FORGE project; i.e. 1) temperatures between 175-225˚C, at 2) depths between 1.5-4.0 km below ground surface, in 3) crystalline rocks, with 4) low permeability, in 5) a stress regime that is favorable for permeability generation through well stimulation, and in 6) a location where there is no existing hydrothermal system. The satisfaction of these criteria as well as the existing infrastructure, necessary safety, data curation, and environment plans, and the involvement of all community stakeholders makes West Flank an ideal location for continuing FORGE activities.

The proposed West Flank site is located ~56 kilometers north of Ridgecrest, CA and ~12 km east of California Route 395, a major highway on the eastern side of Sierra Nevada Mountains (Figure 1). The West Flank site is completely contained within NAWS China Lake, a large and highly secure Navy weapons installation. Required security protocols needed to enter NAWS China Lake and the West Flank will not affect any activities within the site, as site access is facilitated by the Navy GPO on behalf of the NAWS China Lake Command. In total ~4.6 km^2 area is available for development of infrastructure on the FORGE site.

2. GEOLOGIC SETTING

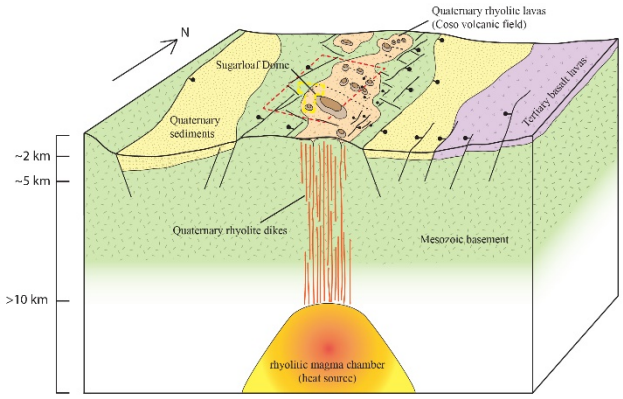

2.1 Regional setting

The proposed West Flank FORGE site lies within the volcanically and tectonically active Coso Range at the boundary between the Sierra Nevada (Sierran) microplate and the Basin and Range. The Sierran block moves ~13 mm/year to the northwest with respect to stable North America. Its motion is accommodated by strike-slip and normal faulting in the Eastern California Shear zone/Walker Lane belt, a ~100 km wide zone of dextral shear deformation along the eastern side of the Sierra Nevada (Stewart, 1988; Faulds et al., 2005).

Figure 2. 3D conceptual model of the area local the West Flank FORGE site (after Duffield and Bacon, 1980).

Regionally, the West Flank site lies in a right step-over between the west-northwest to northwest-striking dextral Airport Lake and Little Lake faults to the south, and the northwest-striking dextral Owens Valley and Wild Horse Mesa faults located north (Figure 1). Within this ~20 km wide step-over with apparent pull-apart geometry, the West Flank FORGE site lies on a horst block consisting of Mesozoic basement rocks. Relative uplift of the horst block is broadly controlled by north-northeast-striking east-dipping normal faults on the east side and north-northeast-striking, west-dipping faults on the west side. These faults, along with west-northwest to northwest-striking dextral-normal faults, step to the left, defining the horst block (Figure 2).

2.2 Local Geologic Setting

The Mesozoic plutonic rocks of the horst block at the West Flank site (Figure 2) are predominantly granitic to dioritic and correlate with the Sierra Nevada Batholith (Duffield et al., 1980; Wilson et al., 2003; Hauksson and Unruh, 2007; Simon et al., 2009). The Mesozoic plutonic rocks intrude felsic metavolcanic and other metamorphic rocks that range from Mesozoic to Precambrian (Duffield and Bacon, 1981; Whitmarsh, 1998a; Whitmarsh, 1998b), though these metamorphic units are not exposed at the surface at West Flank nor are they evident in the eight wells analyzed for lithologic data at West Flank.

Pliocene to Recent volcanic rocks of the Coso volcanic field unconformably overly the Mesozoic basement rocks at the West Flank site (Figure 2). The Coso volcanic field is composed primarily of Pleistocene and younger rhyolite domes, minor basalt flows, and associated volcaniclastic and epiclastic rocks. Rhyolite domes range in age from ~625 ka to ~85 ka (^{40}Ar/^{39}Ar and zircon geochronology; Simon et al., 2009). These youngest domes includes Sugarloaf dome which is the dominant topographic feature at the West Flank (Figure 2 and 3). The magmatic system associated with the Coso volcanic field appears to be maintained by the intrusion of basaltic

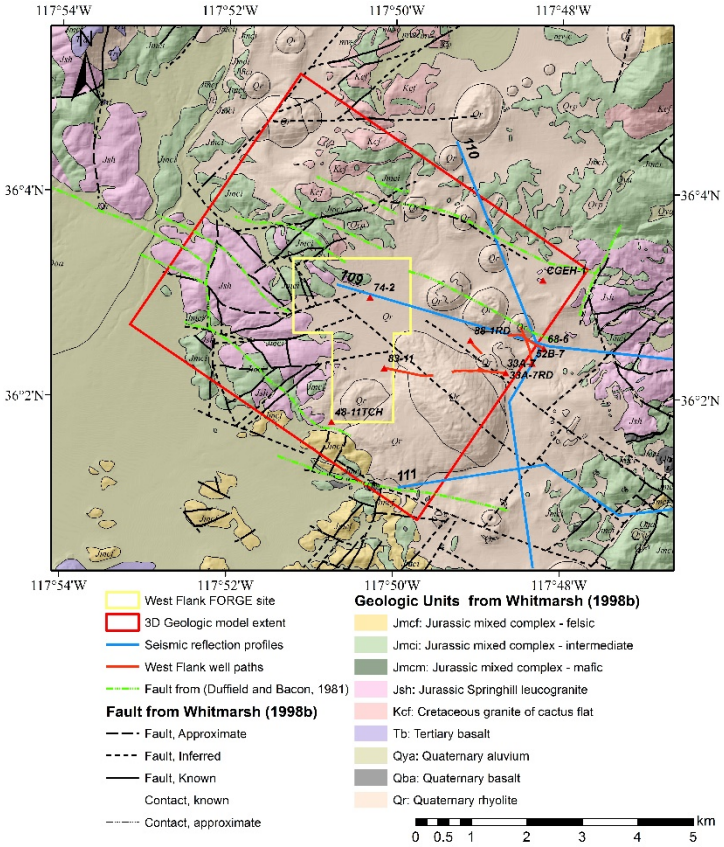

magmas at depth, likely associated with ongoing Basin and Range-style lithospheric extension (Duffield et al., 1980; Manley and Bacon, 2000). The Coso volcanic field magmas where likely derived from partial melting of the crust and/or differentiation these basalt magmas (Duffield et al., 1980; Duffield and Mckee, 1986). The discrete source of the Coso volcanic field lavas is a magma chamber estimated to sit ~11-16 km beneath the West Flank site (Duffield et al., 1980; Hauksson and Unruh, 2007). Dikes sourced from this chamber transported magma to the surface and fed the eruption of the Pliocene to recent rhyolite to basalt lava flows and rhyolite domes (Figure 2). The dikes are predominantly north-northeast striking and steeply dipping, and were intruded along pre-existing north-northeast-striking structures. Conductive heating of the crust associated with the rhyolite magma chamber is responsible for the elevated heat flow at West Flank (Duffield et al., 1980). Overlying the Coso volcanic field deposits is Quaternary sedimentary cover.

Figure 3. Geologic map of the West Flank site. Geologic map after Whitmarsh, 1998a. The proposed West Flank FORGE site is outlined in yellow. The extent of the 3D geologic model is outlined in the red rectangle.

3. SYNTHESIS OF EXISTING DATA

A wide variety of data were synthesized for interpretation of the geologic framework of the West FORGE site, construction of the 3D geologic model, and confirmation of the suitability of the West site for FORGE activities. These data include surface lithologic data, downhole lithologic data, structural data, stress data, thermal data, fluid geochemical data, alteration data, well flow test data, gravity and magnetic data, magnetotelluric data, seismicity and micro-earthquake data, and seismic reflection data. The lithologic data, structural data, stress data, thermal data, and geophysical data will be discussed here, as they directly relate to the geologic framework of the West FORGE site. The geochemistry data, alteration data, and well flow test data, which provide evidence for low permeability, conductive geothermal gradients, and temperature that meet or exceed requisite FORGE parameters, were presented in detail in Sabin et al. (2016) will not be discussed in detail here.

3.1 Lithologic data

Data from the two geologic maps (Duffield and Bacon, 1981, 1:50,000 scale and Whitmarsh 1998b, 1:24,000 scale) were synthesized in order to define the lithologic and structural framework of the West Flank site. These data were utilized as a framework for re-interpretation of the core from well 74-2TCH, the cuttings form wells 83-11 and CGEH-1, and the mud logs from wells 33A-7, 33A-7RD, 88-1RD, 68-6 and 52B-7 (Figure 3).

The mapped surface geology at the West Flank site consists of Quaternary sedimentary deposits and Pleistocene basalt to rhyolite lava flows and domes unconformably overlying Mesozoic plutonic rocks. Quaternary sedimentary deposits (Qa), consist of alluvium and colluvium, form <10 m thick sedimentary cover in the dry washes and basins to the west of the West Flank FORGE site. Underlying the Quaternary sediments, the Pleistocene volcanic units of the Coso volcanic field consist of predominantly rhyolite domes and associated volcaniclastic and epiclastic successions (Qr). The Qr domes and associated volcaniclastic and epiclastic successions occurs as a veneer <500-m-thick, unconformably overlying the Mesozoic plutonic rocks. Dikes sourced from the crustal magma chamber at >11-16 km depth (Duffield et al., 1980; Hauksson and Unruh,

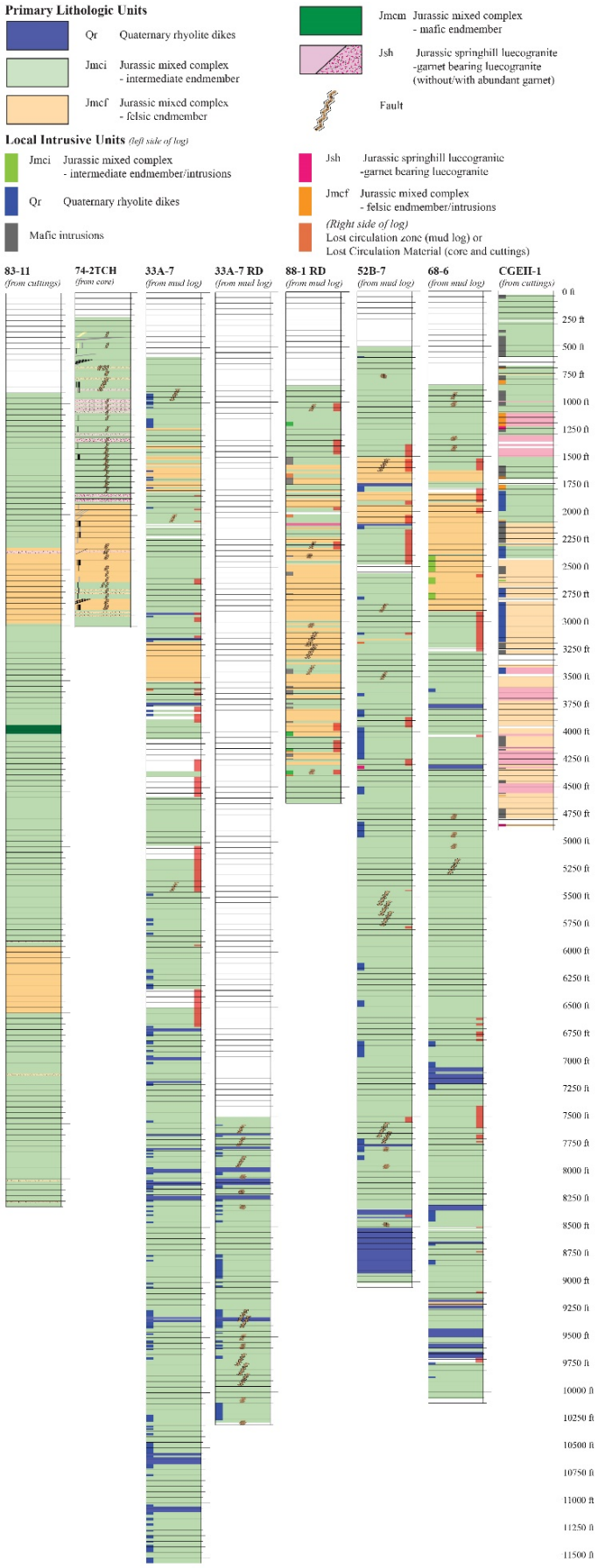

2007)fed the eruption of the rhyolite lava flows and domes. These dikes, the intrusive equivalent of Qr, strike predominantly north-northeast and appear to have been intruded along pre-existing structures (Duffield et al., 1980). Qr dikes are evident in wells 33A-7, 33A-7RD, 52B-7, and 68-6, and occur primarily below ~1,000 m below ground surface (bgs) and in the highest density below ~2,000 m bgs (Figure 4). Mafic intrusions are volumetrically insignificant and their affinity is poorly constrained as a result of several different generations of Mesozoic to Cenozoic mafic eruptive and intrusive rocks that has been mapped throughout the area (Whitmarsh, 1998a, b). Unconformably beneath the Pleistocene rhyolite and Quaternary sediments are Mesozoic granitic to dioritic rocks. These units are exposed throughout the area surrounding the West Flank site and dominate the West Flank subsurface section at depths greater than ~500 m bgs (Figure 4).

Four distinct Mesozoic plutonic units have been identified in the West Flank conceptual model. Diorite to quartz-diorite, the intermediate endmember for the Jurassic mixed intrusive complex (Jmci), is the most volumetrically abundant unit at West Flank. Jmci is defined in hand sample by an assemblage of hornblende, plagioclase ± quartz. Downhole lithologic data from the eight wells analyzed confirm the lateral continuity of Jmci throughout the subsurface of the West Flank site. Jmci is locally intruded by and intermingled with Jmcf, Jurassic granite consisting of plagioclase, alkali feldspar and quartz, with ≤ 10% mafic minerals (primarily muscovite ±biotite) (Whitmarsh, 1998b). Jmcf is the felsic endmember of the Jurassic mixed intrusive complex. Contact relationships between Jmci and Jmcf, as defined in the field and in the 74-2TCH core, are highly diffuse, typically consisting of several meters to tens of meters of mixed and intermingled dikes and/or sills of Jmci, Jmcf, and of compositions intermediate between the two endmembers. Magmatic deformation textures are abundant, confirming that Jmci and Jmcf are likely contemporaneous. In the eight wells analyzed for lithologic data, Jmcf occurs almost exclusively at levels shallower than ~1,350 m and rarely deeper than ~3,000 m bgs (Figure 4).

Figure 4. Lithologic logs of the eight wells used to characterize the subsurface lithology and structure at West Flank of Coso.

The two other Mesozoic plutonic units evident at the West Flank are garnet-bearing, quartz and feldspar leucogranite, which we equate to the Jurassic Springhill leucogranite, Jsh and the Cretaceous quartz and alkali feldspar granite of Cactus Flat, Kcf (Whitmarsh, 1998a). Jsh is found predominately in wells CGEH-1 and 74-2TCH which are adjacent to mapped exposures of Jsh (Figure 3, Whitmarsh, 1998a). Kcf occurs as isolated exposures to the north and west of the West Flank site but was not evident in the lithologic data from any of the eight wells. Petrography and XRD of select cuttings from wells 33A-7, 33A-7RD and 83-11, performed in 2011 by the Energy and Geoscience Institute (EGI) at the University of Utah, confirm these lithologic interpretations and inform on the petrography of the lithologic units and the alteration of in these lithologies. Within the analyzed wells, the clay distribution with depth follows the temperature profile; that is, the occurrence of smectite is coincident with temperatures less than 180˚C, while interlayered smectite-illite or smectite-chlorite is coincident with temperatures between 180˚C and 225˚C and, finally, illite and chlorite is coincident with temperatures above 225˚C (Henley and Ellis, 1983; Reyes, 1990, Clay and Moore, 2013).

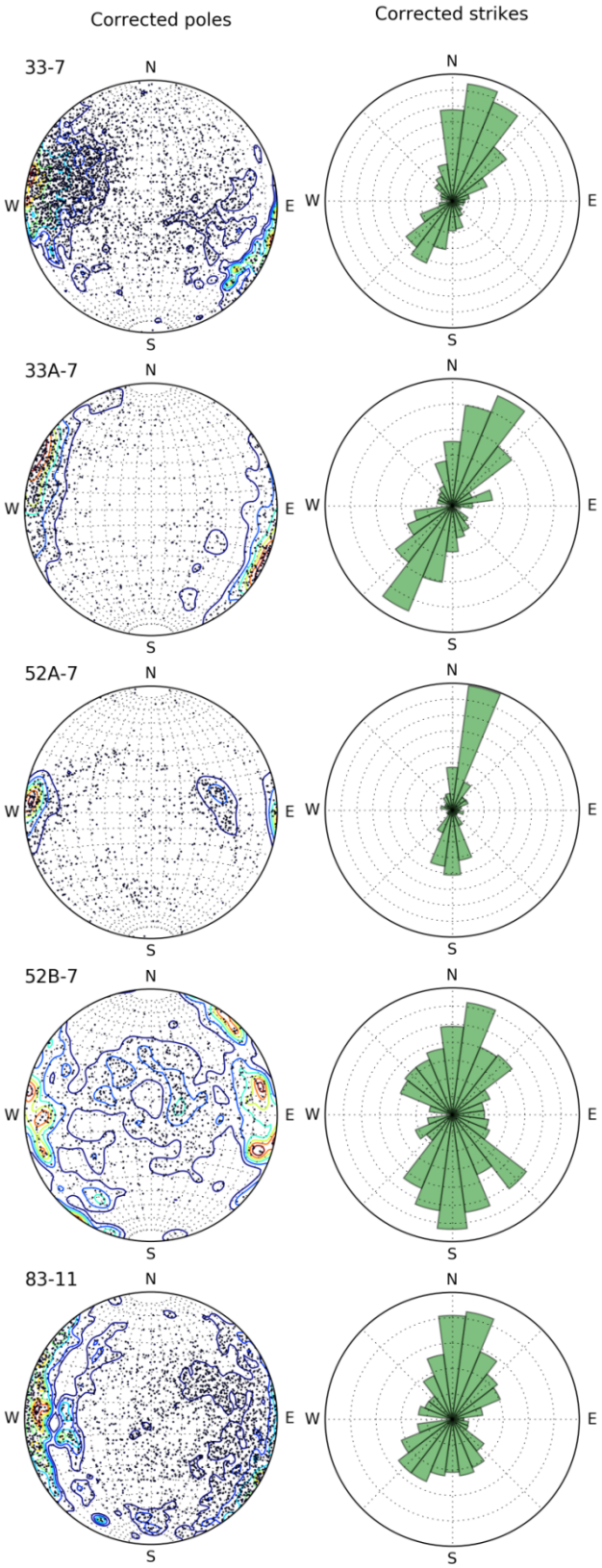

3.2 Structural data

The Duffield and Bacon (1981) and Whitmarsh (1998a) geologic maps were used as constraints on the general structural trends in and around the West Flank site, and on the surface locations and surface geometries of discrete structures (Figure 3). The two primary fault systems area north to north-northeast and west-northwest striking (Bacon et al., 1980; Roquemore, 1980). Inverted focal mechanisms indicate that a north-south to northeast southwest shortening (d3) and an east-west to northwest-southeast extension (d1) is characteristic of the Coso Range-Indian Wells Valley region, and the sub-horizontal orientation of the principal strain components, suggests strike-slip faulting regime. Natural fractures were picked from the image logs of wells 33-7, 33A-7, 52A-7, 52B-7 and 83-11. Where previous analyses of natural fractures were available (GMI [2000, 2001] for wells 33-7, 52A-7, 52B-7), those picks were used. To correct the sampling bias leading to under-sampling of fractures with a steep apparent dip in the wells, a Terzaghi correction was performed (Terzaghi, 1965). With that, each interpreted fracture given a weight by $w=1/\cos(\phi)$, where ϕ is the angle between the wellbore trajectory and the fracture normal. The corrected poles were plotted (Figure 5) with contours as exponential Kamb contours (Kamb, 1959; Vollmer, 1995).

Figure 5 Natural fracture picks from image logs of the FORGE wells. Left column shows 3σ-exponential Kamb contours of poles with applied Terzaghi correction, right column shows the fracture strikes weighted by the Terzaghi correction.

Both the focal mechanism inversion data and the downhole natural fracture data are consistent with mapped structural geometries, confirming that north to north-northeast and west-northwest striking are the two primary structural trends at to West Flank.

3.3 Stress data

Two methodologies were used to characterize the stress field at the West Flank, 1) data from earthquake focal mechanisms, and 2) borehole breakouts and drilling-induced tensile fracture data interpreted from image logs from wells 33-7, 33A-7, 52B-7 and 83-11.

Earthquake focal mechanisms can be classified as normal faulting, strike-slip or thrust faulting based on the geometry of the moment tensor, i.e. the orientation of the tension (T), compression (P) and neutral (B) axes. The focal mechanisms are plotted using ternary diagrams to visualize the position of an earthquake in the spectrum of possible mechanisms (Frohlich, 1992). We use the focal mechanisms catalog by Yang et al (2012) that covers the period from 1981 to 2014 in and around the West Flank site. These data indicate an abundance of strike-slip and trans-tensional mechanisms. Pure normal faulting mechanisms are rare and no thrust faulting mechanisms are observed.

Analyses of wellbore failure data were performed for four wells in and near the West Flank area: 33-7, 33A-7, 52B-7 and 83-11 (Table 1). The complete methodology and results of these analyses are in Schoenball et al. (2016). These analyses indicate that the orientation of S_{Hmax} is spans N0°E-N8°E (Table 1).

Well	*Log type*	*Logged interval [m MD]*	*Typical deviation direction*	*Typical deviation*	*Total length DIFs [m]*	*Total length BOs [m]*	*Total length PCFs [m]*	*Standard deviation [°]*	*SHmax orientation*	*WSM Quality*
33-7	EMI	1886-2806	N340°E	12-25°	40	35	-	21	N5°E	C
33A-7	CBIL	2133-3142	N275°E	29°	71	264	4	17	N8°E	C
52B-7	FMI	2552-2721	N340°E	11°	53	5	-	17	N0°E	B
83-11	CBIL + STAR	604-2097	N100°E	24°	68	9	68	26	N1°E	D

Table 1. Summary of available borehole image logs, interpretation of stress indicators and the inferred stress states. DIF: drilling induced tensile fractures, BO: breakouts, PCF: petal centerline fractures, WSM Quality: World Stress Map quality ranking.

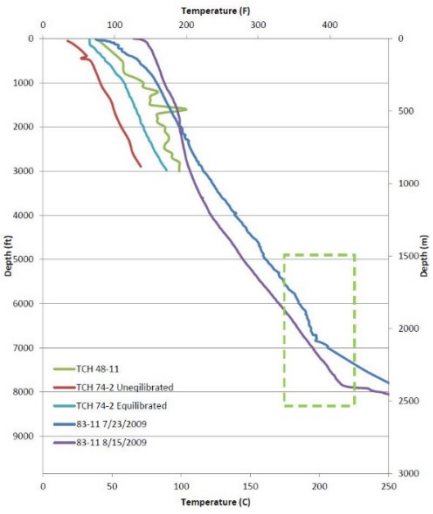

3.4 Thermal data

Within the proposed West Flank FORGE site, three test holes, wells 74-2TCH, 48-11TCH and 83-11, have available temperature data. These data were incorporated into the previously generated temperature model for the Coso geothermal field to the east of the West Flank site, in order to extend the 3D temperature model across the West Flank site. The profiles of these wells demonstrate that within the West Flank site, temperatures above 175˚C occur below ~1700 m depth, well within the 1.5-4 km required for FORGE (Figure 6). The different temperature profiles for 83-11 demonstrate the equilibration and smoothing of the profile (purple) a month after the early survey (blue). The 3D temperature model was constructed based on all the available temperature data from the Coso geothermal field and the West Flank site. The data were contoured using the Kriging method algorithm. The calculated temperatures are anticipated to be within ~6˚C (20˚F), or one contour interval, of the observed data.

Figure 6. Temperature profiles of well 83-11, temperature core hole (TCH) 74-2 and 48-11TCH. Driller's logs indicate basement was encountered at ~600 ft bgs in 83-11. Static temperature profiles in 83-11 were run from July through November 2009 and an injection test was conducted in August 2009. Temperature profiles are thick blue, red and orange lines (48-11TCH). Note that all of the curves are conductive. Interpretations of the injection test on 83-11 suggested that there are no productive (i.e., high permeability) zones in this hole. The green dashed box outlines ideal FORGE temperature conditions in 83-11 between ~1.5 km and 2.5 km bgs.

3.5 Potential field geophysical data

Regional gravity data were collected across the West Flank as part of a study of southern California (Snyder et al., 1981). 136 gravity stations were collected within and surrounding the West Flank FORGE site) with an average spacing of 500 m. Additionally, a higher resolution, local gravity survey across the CVF was collected (Monastero et al., 2005). The survey contains 237 gravity stations within and surrounding the West Flank FORGE site, with an average spacing of 260 m.

A high-resolution aeromagnetic survey was flown over the West Flank (written communication Katzenstein, Monastero, and Jachens). The survey has a line spacing of approximately 540 m with a primary direction of N65E and roughly 10% tie lines. The flight height was ~250 m. The data were corrected for diurnal and atmospheric magnetic variations. The available metadata do not indicate whether the data were leveled or not. The International Geomagnetic Reference Field was subtracted from the data to yield local magnetic anomaly values. The values were then interpolated using a tension spline to generate an estimate of the total magnetic field anomaly. Both the magnetic and the gravity data provide regional coverage of the Coso Range-Indian Wells Valley region and allow us to infer the location of major faults.

3.6 Seismic Reflection data

Forty-five (45) line-km of seismic reflection data were collected in the Coso Range in 2001. The initial analysis and interpretation of these data was performed by Unruh et al. (2001). Optim processed these data by inverting the P-wave first arrivals to create a 2-D velocity structure. Kirchhoff images were then created for each line using velocity tomograms (Unruh et al., 2001). Three of these seismic reflection profiles, lines 109, 110 and 111, are within or proximal to the West Flank FORGE site. Imaging is generally poor as a result of high acoustic attenuation due to the shallow volcanic material and/or low impedance contrasts within the plutonic section. However, the contact between the Pleistocene rhyolite lava flows and domes is evident is all three profiles, as are several faults.

3.7 Magnetotelluric data

Three Magnetotelluric (MT) datasets are available adjacent to and within the West Flank site. The most recent survey, collected in 2011 by Schlumberger/WesternGeco and inverted by the WesternGeco GeoSolutions Integrated EM Center of Excellence in Milan, Italy, expanded the data coverage to the west and covers the West Flank FORGE site. These data were integrated with two earlier surveys, collected in 2003 and 2006 for the present study. A conductive clay cap is visible in the MT data throughout the Coso geothermal field but this low resistivity zone does not to extend into the West Flank. This suggests hydrothermal upflow within the Coso geothermal field with weak outflow toward the West Flank. The lack of conductivity at the West Flank suggests a lack of porosity. This is consistent with petrographic data that demonstrates a lack of fluid flow within veins in 83-11, and with the conductive temperature profile of 83-11. Together these data confirm low permeability and a lack of an existing hydrothermal system at the West Flank.

3.8 Seismicity data

The microseismic network installed at the Coso geothermal field extends beyond the geothermal field, thereby providing coverage of the West Flank FORGE site. The rate of seismicity in the Coso Range-Indian Wells Valley region is very high, with several earthquakes of significant magnitude recorded during the 80 years of seismicity recorded on the USGS Southern California Seismic Network. Several significant earthquakes have occurred in the region. The two largest occurred in 1946 and 1995, M6.3 and M5.8 (which followed a M5.4 earthquake a month prior) respectively. Within the adjacent Coso geothermal field no earthquakes with M>5.0 have been recorded. Earthquakes with M>4.0 have been recorded within the proposed West Flank FORGE site.

The seismicity catalog from April 1996 to May 2012 consists of over 140,000 processed events, including regional events and teleseismic events. Kaven et al. (2014) obtained absolute re-processed locations for a total of 83,790 of these events over from April 1996 to May 2012. A large number of small to moderate seismic events occur in the southeastern portion of the proposed West Flank site. Seismicity generally is restricted to

shallower than ~4-5 km depth and is predominantly microseismicity (M<2.0). This region in the southeastern portion of the West Flank site is separated from the Rose Valley swarm, which has experienced a large amount of naturally occurring seismicity, including some moderate sized earthquakes, by a nearly aseismic region to the west.

4. THE GEOLOGIC FRAMEWORK OF THE FALLON FORGE SITE

In order to assess the distribution and character of potential EGS reservoirs at West Flank, the above data were synthesized into a 3D geologic model encompassing the area within and around the West Flank FORGE site. The model spans ~35 km^2 and is centered on the West Flank site. The 3D geologic model is rotated 35° counterclockwise in order to align with the north-northeast-striking and west-northwest to northwest-striking structural grain. The 3D geologic model extends 6.3 km in the west-northwest dimension and 4.2 km in north-northeast dimension, and extends from the land surface, which varies between ~1075 m asl to ~1650 m asl, to a depth of 2500 m bsl, a total of ~4.1 km. Five 2D geologic cross-sections were constructed to synthesize the map, well, seismic reflection, and microseismicity datasets, and to aid in construction of the 3D geologic model.

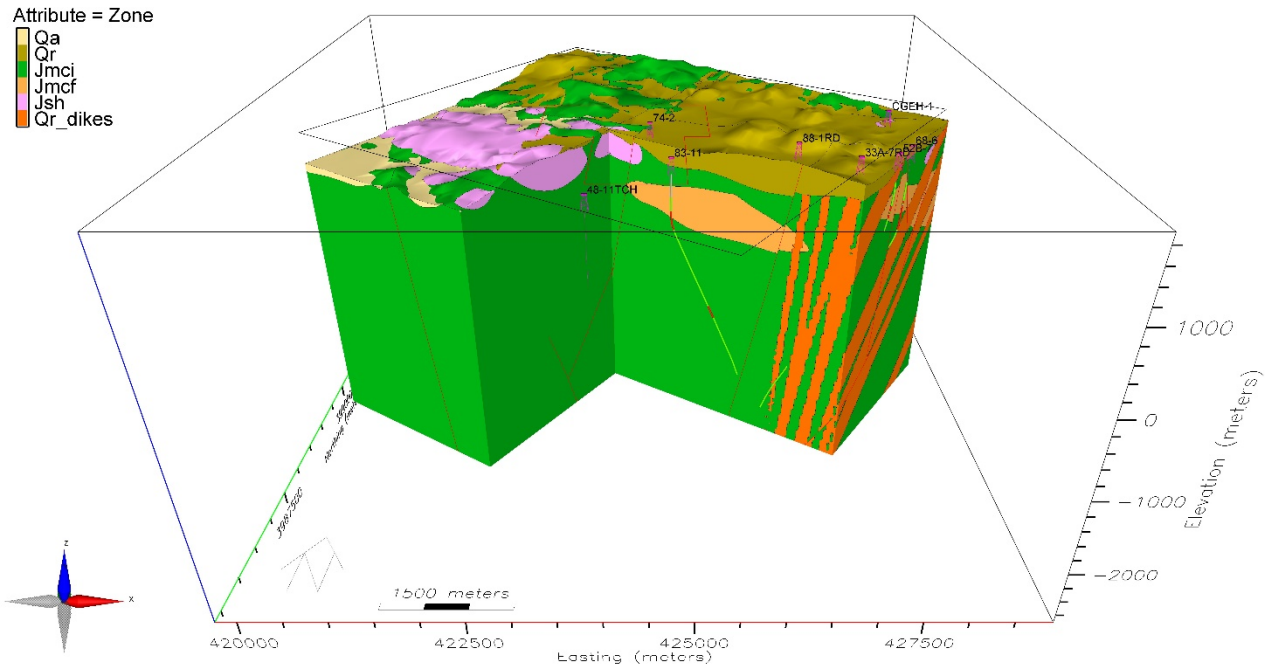

Figure 7. 3D perspective view looking north of the West Flank 3D geologic model sliced through the proposed FORGE site. Well 83-11 is within the West Flank test area footprint.

4.1 Stratigraphic framework

The West Flank FORGE site 3D geologic model consists of six discrete lithologic units, Qa, Quaternary sediments; Qr, Quaternary rhyolite; Qr dikes, Quaternary rhyolite dikes, Jsh, Jurassic Springhill Leucogranite, Jmcf, Jurassic mixed complex-felsic endmember; and Jmci, Jurassic mixed complex-intermediate endmember. Qr and Qa form a veneer, which is < 500 m thick (and more commonly 10s-100m thick) unconformably overlying the Mesozoic plutonic section (Figure 7). At depths greater than ~100 m bgs, the 3D geologic model consists of exclusively crystalline rock; Jurassic granitic rocks (Jmci, Jmcf and Jsh) and Quaternary rhyolite dikes (Qr). Diorite to quartz-diorite, Jmci, is by far the most abundant lithologic unit at West Flank. Jmci constitutes ~88% of the interpreted rock volume of the West Flank 3D geologic model. Jmcf, Jurassic granite is modeled as one intrusion into Jmci, which is ~800 m thick, extending ~3 km x 3 km in the center to northeast corner of the 3D geologic model. The Jurassic Springhill leucogranite, Jsh, occurs as two discrete intrusions, in the southwest and northeast of the 3D geologic model. Both Jsh intrusions are ~500 m thick. Qr dikes, the feeder for the Qr lava flows and domes, occur as discrete, tabular, steeply dipping dikes on the eastern side of the 3D geologic model (Figure 7).

4.2 Structural framework

The 3D geologic model includes eight faults, their locations and geometry constrained by a combination of geologic maps, geologic cross-sections, seismic reflection interpretation, the locations of known faults in core, the location major zones of lost circulation during drilling, the occurrence of lost circulation material in core and well cuttings, borehole image (structural) data from the eight wells, and microseismicity data. Five of the modeled faults strike north to northeast and three faults strike west to west-northwest. These orientations are consistent with the general regional structural trends and down-hole natural fracture data.

4.3 Uncertainty in 3D geologic interpretations

The relative uncertainty in the 3D geologic interpretations was calculated based on relative distance from the input datasets. The primary input datasets utilized for constraining the subsurface 3D geologic geometry are the geologic cross-sections, geologic maps, lithologic logs along well paths, and seismic reflection profiles. The distance between and the locations of these datasets and all locations within the 3D geologic model were calculated. Relative uncertainty was calculated by fitting the distances to a logarithmic relative uncertainty curve (Figure 8). At locations very near to input data, relative uncertainty in the 3D model is very low (high confidence in the geologic interpretation). With increasing distance from each input dataset, relative uncertainty increases progressively.

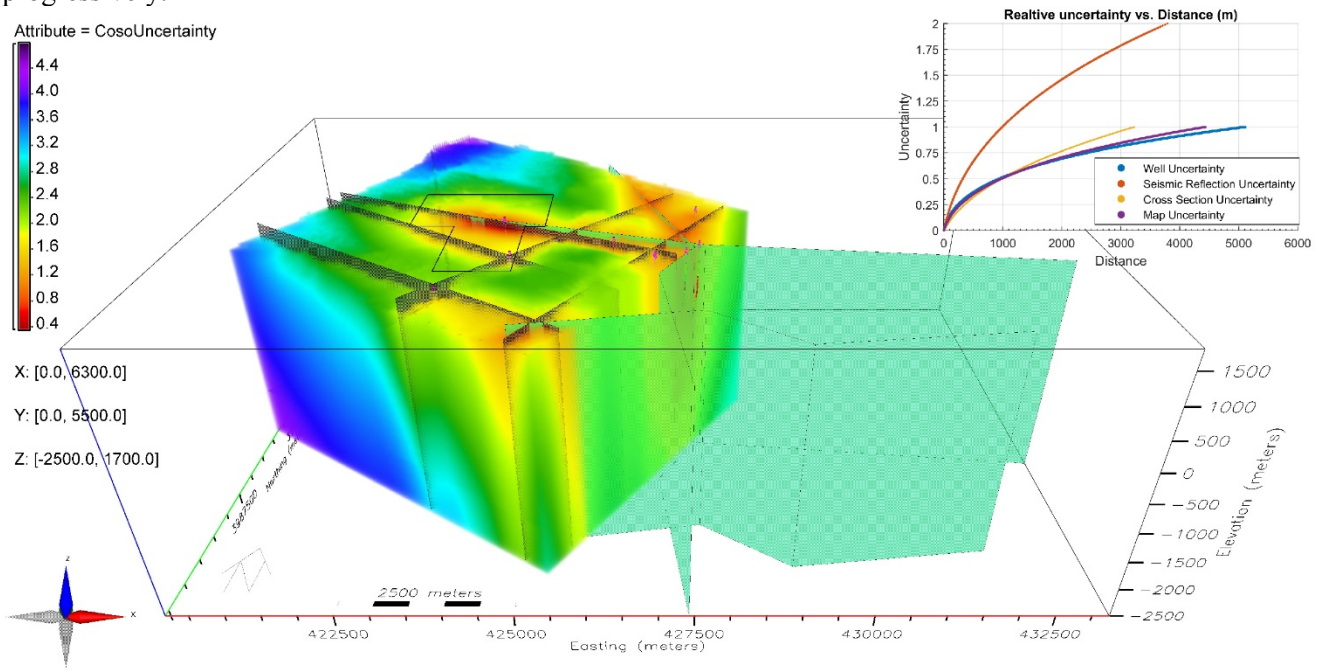

Figure 8. Relative uncertainty in the 3D geologic interpretations based on distance from the input data. Geologic cross sections shown as black planes, seismic reflection profiles shown as green planes, and the wells with lithologic data shown in pink. Warm colors correspond to relatively low uncertainty in the 3D modeled results.

Past a distance of 1 km, which is the mean spacing of the eight wells used for lithologic analyses and the mean spacing of the geologic cross-sections, the progressive increase in relative uncertainty with distance lessens; that is, the input data are probably too distant to make confident geologic interpretations and therefore the relative uncertainty is already high and cannot further increase. Relative uncertainty between zero and one was calculated for the eight wellbores with lithologic data, the geologic map, and the geologic cross-sections. Since constraining the Mesozoic basement geology is central to this effort, only the distance from mapped basement exposures was calculated. As a result of poor resolution, we have lower confidence in the seismic reflection interpretation than the other input data sets, so the relative uncertainty based on the seismic reflection interpretation was calculated between 0 and 2 with a distance of 1 km set to a relative uncertainty of 1 (Figure 8). The relative uncertainty volumes for all the input datasets were summed to produce a cumulative relative uncertainty for a 3D volume for which the 3D geologic model was constructed (Figure 8). The relative uncertainty analysis indicates that as a result of a high density of data, we have relatively high confidence in the modeled geologic relationships within

the West Flank FORGE site. We also have relatively high confidence in the modeled geologic relationships directly to the east of the West Flank site. However, to the north and of the West Flank site an absence of downhole lithologic data and seismic reflection data limit our confidence in the modeled geologic relationships.

4.4 Conditions for reservoir engineering at West Flank

Temperature logs indicate that the 175-225°C temperature window required for FORGE is spans ~1.7-2.4 km bgs in well 83-11 (Figure 6). Temperature modeling, incorporating data from within the Coso geothermal field, and data from wells 83-11, 74-2TCH and 48-11TCH confirms that the 175-225°C temperature window occurs at these depths, ~1.7-2.4 km bgs, throughout the West Flank site (Figure 9). Within this temperature and depth window, extending to 2500 m depth or ~4100 m bgs (the base of the geologic model), ~14 km^3 of weakly altered to unaltered diorite to quartz-diorite Jmci, granitic Jmcf, and Qr rhyolite dikes occur (Figure 9 and Table 2). This volume of rock that lies within the FORGE parameters at West Flank, consists of ~12.5 km^3 of crystalline rock and is ~85%, unaltered diorite to quartz-diorite Jmci formation and ~1.5 km^3, or ~15%, Qr, Quaternary rhyolite dikes.

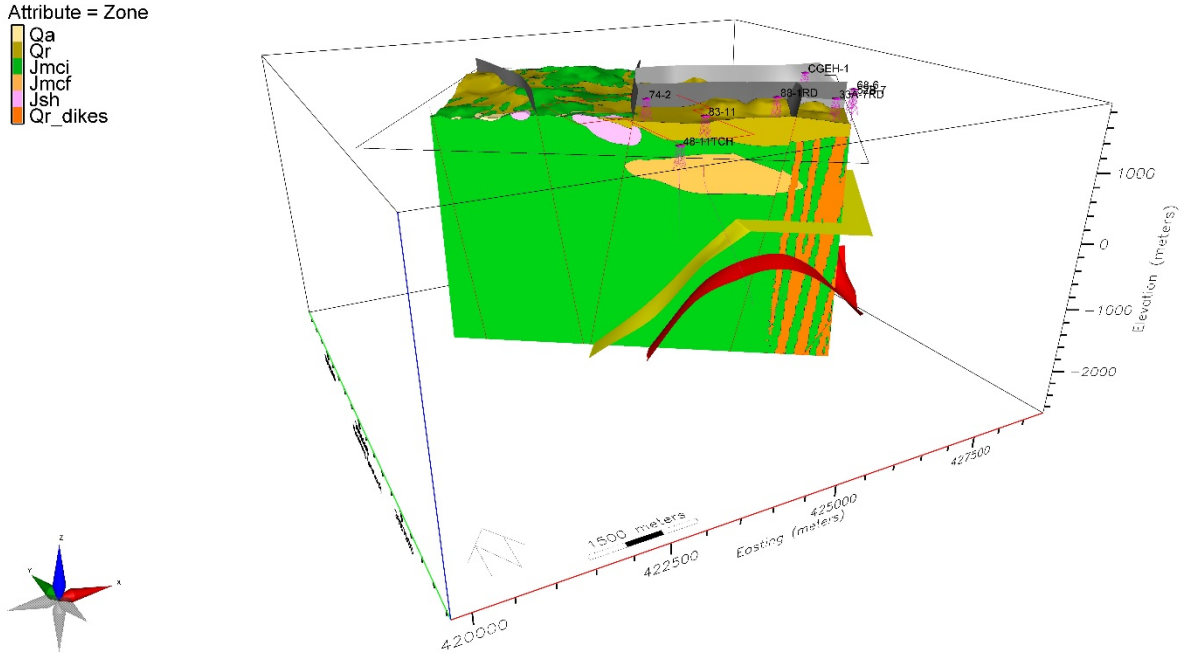

Figure 9. Oblique north-east looking view of the West Flank 3D geologic model. The 175°C isotherm surface is yellow and truncated at 1.5 km beneath the ground surface and the 225°C isotherm surface is red. The modeled volume of crystalline rock within the temperature window, extending to 2.5 km bsl (the base of the model) is 14 km^3, ~2.5 km^3 of crystalline rock lie within this temperature window and within the vertically extended footprint of the West Flank FORGE site.

	Total Model Volume (km^3)	Total model volume within FORGE site (km^3)	Total Model Volume between 175-225°C (km^3)	Model volume within FORGE site between 175-225°C (km^3)
All units	131.28	17.37	14.00	2.47
Qa	0.07	-	-	-
Qr	2.73	-	-	-
Qr dikes	6.30	-	1.44	-
Jmci	4.50	16.56	12.56	2.47
Jmcf	1.71	0.47	-	-
Jsh	115.97	0.35	-	-

Table 2. Volume of the geologic model and each of the 6 modeled lithologic units. Column 1, total modeled volume (~35 km^2 areal extent). Column 2 modeled volumes within the West Flank Site (4.6 km^2 areal extent), Column 3 modeled volumes falling within 175-225°C within the 3D model volume. Column 4 modeled volumes within the West Flank Site and falling within 175-225°C. All volumes calculated to a depth of -2500 m bsl or ~3800 m bgs.

Based on slip and dilation tendency analysis, we infer the orientations of structures that are most likely to become reactivated during a hydraulic stimulation (Morris et al., 1996; Ferrill et al., 1999). Based on these analyses, the existing natural fault and fracture systems at West Flank are well oriented with respect to the measured stress conditions for reactivation during well stimulation (Figure 10).

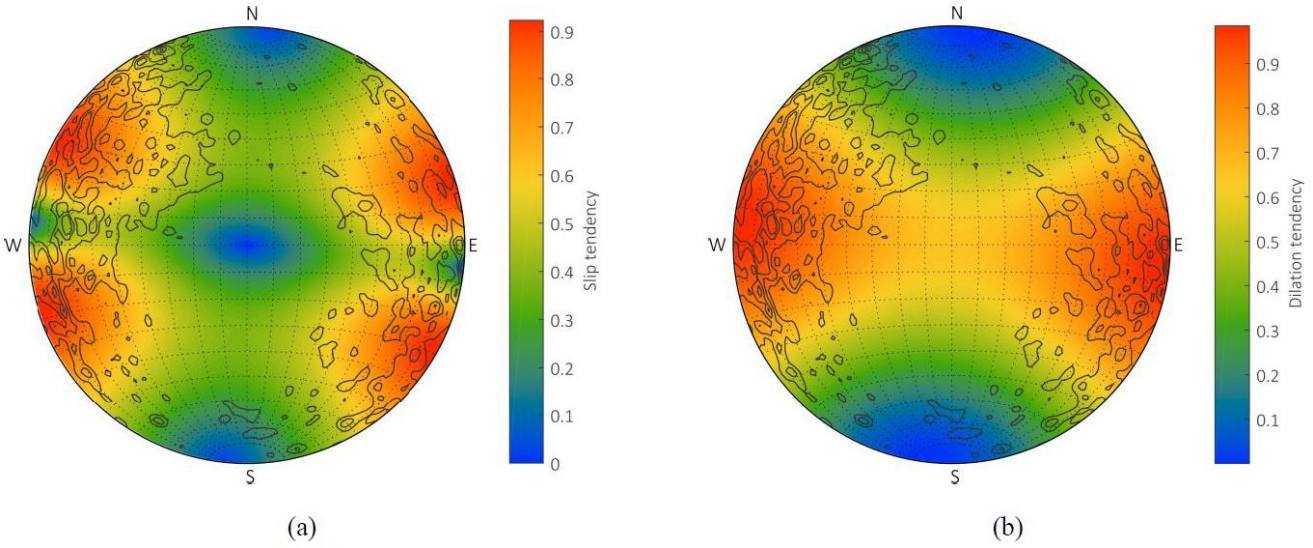

Figure 10. (a) Slip tendency and (b) dilation tendency for fracture normal for the preferred stress model with SHmax = 44 MPa/km. Terzaghi-corrected 3σ-Kamb contours of natural fractures from West Flank wells (same as Figure 5) are superimposed.

5. CONCLUSIONS

Evaluation and synthesis of the multiple geologic and geophysical data sets have facilitated the development of the 3D geologic model of the proposed West Flank FORGE site. These analyses permit confirmation that the West site satisfies each major qualifying criteria for FORGE and represents and ideal candidate for future FORGE activities.

1) Temperature: Well temperature data provide direct evidence that temperatures at the West Flank FORGE site are within the specified 175 to 225°C range. Well 83-11 reaches 175°C at ~1700 m bgs (Figure 5). Based on the 3D geologic model, we demonstrate that there is ~2.5 km^3 of crystalline rock at depths of 1.5 to 2.5 km bgs in this temperature range within the boundaries of the FORGE site (Figure 9 and Table 2).

2) Low Permeability: Well-test data provide direct evidence for low permeability conditions at the West Flank FORGE site. Air and water lifts and an injection test were performed on 83-11 after the well was completed. These tests demonstrated a buildup of pressure in the wellbore during injection testing and a lack of flow during the air lift suggesting very low permeability. The result of the well testing determined that the well was non-commercial and with low permeability.

3) Crystalline rock: Analyses of cuttings, core and thin sections from wells in the West Flank FORGE site demonstrates that the subsurface at West Flank is composed almost entirely of crystalline basement rock. Mesozoic plutonic rocks dominate with smaller volumes of Quaternary rhyolite dikes (Table 2). Geologic mapping in the West Flank area (Figure 3) confirms the ages and areal extent of these lithologic units, an assemblage of Jurassic and Cretaceous plutons, sills and dikes, all locally cut or overlain by flows, domes and dikes associated with the <1.0 Ma Coso Volcanic Field.

4) Depth (1.5-4.0 km): Data from wells drilled in the West Flank provide direct evidence that required FORGE temperatures can readily be found in crystalline basement rock between 1.5 and 4.0 km depths (Figures 4, 6, 9 and Table 2).

5) Favorable stress regime for stimulation: Stress data, structural data, and seismicity data confirm that the West Flank FORGE site are characterized by trans-tensional stress conditions that are conducive to for EGS success. These data indicate that the existing natural fracture system is well oriented with respect the measured stress field, for stimulation (Table 1 and Figure 10).

6) Not in and active hydrothermal system: The 83-11 static temperature profile illustrates a conductive heat flow (Figure 5). Well tests on 83-11 indicate that it is non-commercial with very low permeability. Subsequent pressure monitoring data comparing 83-11 downhole pressure over time with wells in the Coso hydrothermal field to the east, indicate that there is no pressure connection between 83-11 and the hydrothermal field. Cuttings, core, and thin sections from 83-11 and 74-2TCH (Figure 4) demonstrate a locally fractured and faulted crystalline basement with no mineralogical indications of contemporary hydrothermal alteration. MT data suggest that the low resistivity "clay cap," which is prominent in the Coso hydrothermal system to the east, does not extend to the West Flank. Collectively, all of these relationships confirm that it is very unlikely that an active hydrothermal system resides within the proposed West Flank FORGE site.

ACKNOWLEDGEMENTS

This project is funded by a Department of Energy grant EE0007156 awarded to the FORGE team, with Sandia National Laboratory as lead on the project. The FORGE team acknowledges the support of the U.S. Navy and the Bureau of Land Management for the use of their land and their support in ongoing and proposed future phases of this project.

REFERENCES

Bacon, C.R., Duffield, W.A., and Nakamura, K., 1980, Distribution of Quaternary Rhyolite Domes of the Coso Range, California: Implications for Extent of the Geothermal Anomaly: Journal of Geophysical Research, v. 85, no. 9, p. 2425–2433.

Duffield, W.A., and Bacon, C.R., 1981, Geologic Map of the Coso Volcanic field and adjacent areas, Inyo County, California. United States Geological Survey, scale 1:62,500:.

Duffield, W.A., Bacon, C.R., and Dalrymple, G.B., 1980, Late Cenozoic volcanism, geochronology, and structure of the Coso Range, Inyo County, California: Journal of Geophysical Research, v. 85, no. B5, p. 2381, doi: 10.1029/JB085iB05p02381.

Duffield, W.A., and Mckee, E.H., 1986, Geological Society of America Bulletin northeastern California Geochronology, structure, and basin-range tectonism of the Warner Range, northeastern California: , doi: 10.1130/0016-7606(1986)97<142.

Faulds, J.E., Henry, C.D., and Hinz, N.H., 2005, Kinematics of the northern Walker Lane: An incipient transform fault along the Pacific–North American plate boundary: Geology, v. 33, no. 6, p. 505–508, doi: 10.1130/G21274.1.

Ferrill, D.A., Winterle, J., Wittmeyer, G., Sims, D., Colton, S., Armstrong, A., Horowitz, A.S., Meyers, W.B., and Simons, F.F., 1999, Stressed rock strains groundwater at Yucca Mountain , Nevada: GSA Today, v. 9, no. 5, p. 2–9.

Frohlich, C., 1992, Triangle diagrams: ternary graphs to display similarity and diversity of earthquake focal mechanisms: Physics of the Earth and Planetary Interiors, v. 75, no. 1-3, p. 193–198, doi: 10.1016/0031-9201(92)90130-N.

Hauksson, E., and Unruh, J., 2007, Regional tectonics of the Coso geothermal area along the intracontinental plate boundary in central eastern California: Three-dimensional Vp and Vp/Vs models, spatial-temporal seismicity patterns, and seismogenic deformation: Journal of Geophysical Research: Solid Earth, v. 112, no. 6, doi: 10.1029/2006JB004721.

Kaven, J.O., Hickman, S.H., and Davatzes, N.C., 2014, Micro-seismicity and seismic moment release within the

Coso Geothermal Field, California: Thirty-Ninth Workshop on Geothermal Reservoir Engineering Stanford University, v. 39, p. 10.

Manley, C.R., and Bacon, C.R., 2000, Rhyolite Thermobarometry and the Shallowing of the Magma Reservoir, Coso Volcanic Field, California: Journal of Petrology, v. 41, no. 1, p. 149–174, doi: 10.1093/petrology/41.1.149.

Monastero, F.C., Katzenstein, A.M., Miller, J.S., Unruh, J.R., Adams, M.C., and Richards-Dinger, K., 2005, The Coso geothermal field: A nascent metamorphic core complex: Bulletin of the Geological Society of America, v. 117, no. 11-12, p. 1534–1553, doi: 10.1130/B25600.1.

Morris, A., Ferrill, D.A., and Henderson, D.B., 1996, Slip-tendency analysis and fault reactivation: Geology, v. 24, no. 3, p. 275–278.

Roquemore, G., 1980, Structure, tectonics and stress field of the Coso Range, Inyo County, California: Journal of Applied Geophysics, v. 85, no. B5, p. 2434–2440.

Sabin, A., Blake, K., Lazaro, M., Meade, D., Blankenship, D., Kennedy, M., Mcculloch, J., Deoreo, S., Hickman, S., Glen, J., Kaven, O., Schoenball, M., Williams, C., Phelps, G., et al., 2016, Geologic setting of the West Flank, a FORGE site adjecent to teh Coso Geothermal Field, *in* Proceedings, Forty-first Workshop on Geothermal Reservoir Engineering, Stanford University, p. 14.

Schoenball, M., Glen, J.M.G., and Davatzes, N.C., 2016, Analysis and Interpretation of Stress Indicators in Deviated Wells of the Coso Geothermal Field: 41st Workshop on Geiothermal Reservoir Engineering, v. 41, p. 12.

Simon, J.I., Vazquez, J.A., Renne, P.R., Schmitt, A.K., Bacon, C.R., and Reid, M.R., 2009, Accessory mineral U-Th-Pb ages and 40Ar/39Ar eruption chronology, and their bearing on rhyolitic magma evolution in the Pleistocene Coso volcanic field, California: Contributions to Mineralogy and Petrology, v. 158, no. 4, p. 421–446, doi: 10.1007/s00410-009-0390-9.

Snyder, D.B., Roberts, C.W., Saltus, R.W., and Sikora, R.., 1981, Magnetic tape containing the principal facts of 64,402 gravity stations in the State of California:.

Stewart, J.H., 1988, Tectonics of the Walker Lane belt, western Great Basin: Mesozoic and Cenozoic deformation in a zone of shear, *in* Ernst, W.G. ed., Metamorphism and crustal evolution of the western United States, Prentice-Hall, Englewood Cliffs, New Jersey, p. 683–713.

Unruh, J., Pullammanappallil, S.K., Honjas, W., and Monastero, F.C., 2001, New seismic imaging of the Coso geothermal field, eastern California, *in* Geothermal Research Council Transactions, p. 7.

Whitmarsh, R.S., 1998a, Geologic map of the Cactus Peak 7.50 quadrangle; Inyo County, California. Scale 1:24,000:.

Whitmarsh, R.S., 1998b, Structural development of the Coso Range and adjacent areas of east-central California; unpublished PhD Thesis: University of Kansas.

Wilson, C.K., Jones, C.H., and Gilbert, H.J., 2003, Single-chamber silicic magma system inferred from shear wave discontinuities of the crust and uppermost mantle, Coso geothermal area, California: Journal of Geophysical Research, v. 108, no. B5, p. 2226, doi: 10.1029/2002JB001798.

Yang, W., Hauksson, E., and Shearer, P.M., 2012, Computing a large refined catalog of focal mechanisms for southern California (1981-2010): Temporal stability of the style of faulting: Bulletin of the Seismological Society of America, v. 102, no. 3, p. 1179–1194, doi: 10.1785/0120110311.